

Original Article

# iASPP protects the heart from ischemia injury by inhibiting p53 expression and cardiomyocyte apoptosis

Timur Yagudin<sup>1,3,†</sup>, Yue Zhao<sup>1,†</sup>, Haiyu Gao<sup>1</sup>, Yang Zhang<sup>1</sup>, Ying Yang<sup>1</sup>, Xiaofang Zhang<sup>1</sup>, Wenbo Ma<sup>1</sup>, Tolessa Muleta Daba<sup>1</sup>, Vladimir Ishmetov<sup>1,4</sup>, Kai Kang<sup>2</sup>, Baofeng Yang<sup>1</sup>, and Zhenwei Pan<sup>1,\*</sup>

<sup>1</sup>Department of Pharmacology (The Key Laboratory of Cardiovascular Research, Ministry of Education) at College of Pharmacy, Harbin Medical University, Harbin 150086, China, <sup>2</sup>Department of Cardiovascular Surgery, The First Affiliated Hospital of Harbin Medical University, Harbin 150001, China, <sup>3</sup>Department of Hospital Surgery, Bashkir State Medical University, Ufa 450008, Russian Federation, and <sup>4</sup>Department of Cardiovascular Surgery in Clinic, Hospital of Bashkir State Medical University, Ufa 450059, Russian Federation

<sup>†</sup>These authors contributed equally to this work.

\*Correspondence address. Tel: +86-451-86671354; Fax: +86-451-86675769; E-mail: [panzw@ems.hrbmu.edu.cn](mailto:panzw@ems.hrbmu.edu.cn)

Received 9 March 2020; Editorial Decision 11 May 2020

## Abstract

Currently, there remains a great need to elucidate the molecular mechanism of acute myocardial infarction in order to facilitate the development of novel therapy. Inhibitor of apoptosis-stimulating protein of p53 (iASPP) is a member of the ASPP family proteins and an evolutionarily preserved inhibitor of p53 that is involved in many cellular processes, including apoptosis of cancer cells. The purpose of this study was to investigate the possible role of iASPP in acute myocardial infarction. The protein level of iASPP was markedly reduced in the ischemic hearts *in vivo* and hydrogen peroxide-exposed cardiomyocytes *in vitro*. Overexpression of iASPP reduced the infarct size and cardiomyocyte apoptosis of mice subjected to 24 h of coronary artery ligation. Echocardiography showed that cardiac function was improved as indicated by the increase in ejection fraction and fractional shortening. In contrast, knockdown of iASPP exacerbated cardiac injury as manifested by impaired cardiac function, increased infarct size, and apoptosis rate. Mechanistically, overexpression of iASPP inhibited, while knockdown of iASPP increased the expressions of p53 and Bax, the key regulators of apoptosis. Taken together, our results suggested that iASPP is an important regulator of cardiomyocyte apoptosis, which represents a potential target in the therapy of myocardial infarction.

**Key words:** iASPP, myocardial infarction, apoptosis, p53

## Introduction

Acute myocardial infarction (AMI) is currently one of the leading causes of mortality in developed countries [1]. Over the past 20 years, significant advances have been made in the prevention and acute phase treatment of myocardial infarction (MI). However, the mortality rate after MI remains high because of myocardial cell apoptosis and necrosis due to an increase in the concentration of oxygen free radicals and calcium overload of myocardial cells.

When the ischemic myocardial tissue is restored to perfusion, the patient develops a series of symptoms of reperfusion injury, such as arrhythmia, infarct size enlargement, and eventually leading to cardiac insufficiency [2]. Several studies have demonstrated that apoptosis plays an important role in the development of cardiac dysfunction after MI [3].

Apoptosis is a very complex process. The apoptosis-stimulating protein p53 participates in cell cycle control, DNA repair [4,5],

apoptosis [6], and cell stress response as a transcription factor. It induces apoptotic mechanisms via upregulation of Bax transcription [7]. It was found that inhibiting the *Bax* gene and then blocking the p53 apoptosis pathway could protect the heart from ischemic injury. Inhibitor of apoptosis stimulating protein of p53 (iASPP) is the third member of the ASPP family (encoded by the *PPP1R13L* gene) that is the most conserved inhibitor of p53-mediated apoptosis. Previous studies have shown that iASPP is expressed predominantly in the heart, placenta, and prostate, but feebly expressed in the brain, liver, skeletal muscle, testis, and peripheral blood leukocyte [8]. Some studies also showed that the function of iASPP is to prevent apoptosis [9,10]. The functions of iASPP's in apoptosis are fulfilled by binding with p53 and inhibiting its transactivation function on the promoters of pro-apoptotic genes [11,12]. Overexpression of iASPP was observed in different types of human cancers, such as breast carcinoma, acute leukemia, hepatocellular carcinoma, and lung cancer [13–17]. Interestingly, iASPP deficiency caused by spontaneous mutation has been reported to be associated with a lethal autosomal recessive cardiomyopathy in Poll Hereford calves [18,19] and Wa3 mice [20]. However, the regulatory effect of iASPP on cardiac apoptosis remains unclear. We hypothesized that iASPP may play an important role in the pathogenesis of myocardial injury by regulating p53 and apoptosis.

In this study, we performed both *in vivo* and *in vitro* experiments to explore the role of iASPP in cardiac injury and the underlying mechanism. We for the first time discovered that the expression level of iASPP was downregulated in heart tissues following MI stimulation. Overexpression of iASPP improved cardiac function and reduced infarct size in cardiac infarction mice. Our results demonstrated that iASPP is a critical regulator in cardiac infarction.

## Materials and Methods

### Animals

All animal studies were approved by the Institutional Animal Care and Use Committee of Harbin Medical University. All animals care and experimental procedures were in accordance with the regulations of the Institutional Animal Care and Use Committee of Harbin Medical University. All animals were housed in an environment with filtered air, uniform temperature (21–23°C), and humidity between 55% and 65%, in a light-controlled room with food and water available *ad libitum*.

### Animal model of MI

Adult C57BL/6 male mice (8–10 weeks old) were provided by the Animal Center at the Second Affiliated Hospital of Harbin Medical University (Harbin, China). MI model was established as described previously [21,22]. Briefly, after 2 weeks of AAV9 injection through the tail vein, mice were anesthetized with a cocktail of ketamine, xylazine, and atropine (100 mg/kg, 10 mg/kg, and 1.2 mg/kg, respectively, *i.p.*), and then intubated and ventilated with UGO Basile 28025 Mouse Ventilator (respiratory rate: 100/min, respiratory volume: 0.5 ml). A left thoracotomy in the third intercostal space was performed to expose the heart. Left anterior descending branch (LAD) below the tip of the left auricle was tied with a 7-0 sterile silk suture. Sham subjects underwent the same operation except for LAD ligation. After the operation, echocardiography was performed, and hearts were collected and prepared for the subsequent experiments.

### Echocardiography to examine heart function

Echocardiographic studies were performed after the mice were anesthetized as described earlier. Left ventricle (LV) functions were assessed by two-dimensional guided M-mode echocardiography with a 15-MHz linear array transducer system (Vevo 2100 Imaging system; Visual Sonics, Toronto, Canada). The dimensions of the left ventricular cavity were measured, and the percentage change of the fractional shortening (FS) was calculated as:  $FS (\%) = [(LVEDD - LVESD) / LVEDD] \times 100\%$ , where LVEDD is LV end-diastolic diameter and LVESD is LV end-systolic diameter. The LV ejection fraction (EF) was calculated as:  $EF (\%) = [(EDV - ESV) / EDV] \times 100\%$ , where EDV is the LV volume at end-diastole and ESV is the LV volume at end-systole. The volume of the LV was estimated by the area-length method [23].

### Measurement of infarct size

The infarct size was measured by 2,3,5-triphenyltetrazolium chloride (TTC) staining. Briefly, The hearts were rapidly removed from the anesthetized mice, and the pre-cooled PBS was used to wash away the residual blood. After the hearts had been taken out, they were sliced into smaller slices of myocardia (1 mm) along the vertical direction of the LVs. Next, the myocardium slices were first immersed in pre-warmed 1% TTC solution (37°C) and incubated at 37°C for 30 min in the dark, during which the areas of necrosis appeared to be grayish-white. The stained myocardial sections were then placed on the microscopy scanner (Microscopy GmbH 37081; Carl Zeiss, Göttingen, Germany). The infarct area (IA), noninfarct area, and whole LV were measured and calculated using the computer morphometric software Image J (NIH, Bethesda, USA).

### Neonatal cardiomyocyte isolation and culture

Neonatal mice cardiac myocytes (NMCs) were prepared as described previously [24]. The cells were cultured in Dulbecco's modified Eagle medium (Biological Industries, Kibbutz Beit-Harmek, Israel), supplemented with 20% fetal bovine serum (Biological Industries), streptomycin (100 U/ml; Biological Industries), and penicillin (100 U/ml; Biological Industries), and were grown in a humidified CO<sub>2</sub> incubator with 5% CO<sub>2</sub> at 37°C. The cells were seeded into 6-well culture plates at a density of  $1 \times 10^6$  cells per well and cultured for 48 h. Then, the cells were exposed to 200 nM hydrogen peroxide for 12 h.

### Synthesis and transfection of iASPP constructs for overexpression and knockdown

iASPP-specific siRNA and a negative control siRNA were commercially synthesized by Ribobio (Guangzhou, China). The sequences of iASPP-specific siRNA were as follows: sense 5'-GCAUGGGA CUGAUGCACAA-3' and antisense 5'-UUGUGCAUCAGUCCCA UGC-3'. The sequences of negative control siRNA were sense 5'-UUCUCCGAACGUGUCACGUTT-3' and antisense 5'-ACGU GACACGUUCGGAGAATT-3'. These constructs were transfected into cells for iASPP knockdown at a final concentration of 100 nM. iASPP cDNA was inserted into the pCDNA3.1, and the plasmid vectors were transfected into cells for iASPP overexpression at a final concentration of 2.5 mg/l. The transfection was performed using X-treme GENE Transfection Reagent (Roche, Basel, Switzerland) according to the manufacturer's instructions. Forty-eight hours after transfection, the cardiomyocytes were collected for total RNA isolation or protein extraction.

### Construction of adenovirus carrying iASPP and gene delivery *in vivo*

Adenovirus vectors carrying iASPP (OE-iASPP) or a short RNA fragment for silencing iASPP (Si-iASPP) were constructed by Cyagen Co., Ltd (Guangzhou, China). OE-iASPP, Si-iASPP, or control constructs was administered into C57BL/6 mice via tail vein injection at  $1 \times 10^9$  genome containing particles (GC)/animal in 100  $\mu$ l volume. Two weeks after injection, the mice were subject to data collection.

### Terminal transferase-mediated dUTP nick end labeling staining

Terminal transferase-mediated dUTP nick end labeling (TUNEL) staining was performed using an *in situ* cell death detection kit (Roche) according to the manufacturer's instructions. The study was conducted with cardiac tissues according to the standard protocol. Briefly, the paraffin-embedded cardiac tissues were cut into 5- $\mu$ m-thick slices, deparaffinized, and rehydrated. After being penetrated in proteinase K (10  $\mu$ g/ml), the slices were blocked in goat serum fast blocking buffer and incubated in reaction buffer containing enzyme in the dark. The nuclei were counterstained with DAPI. The slices were washed three times with PBS buffer (5 min each). For cardiomyocyte staining, cultured cells were fixed on glass slides and stained with the same procedures used in tissues slices. Sections were examined under the fluorescence microscope (Carl Zeiss).

### Lactate dehydrogenase assay

To determine the cardiomyocyte injury induced by hydrogen peroxide ( $H_2O_2$ ), the release of lactate dehydrogenase (LDH) was detected. In general, LDH is retained in the cytoplasmic fraction but is released into the surrounding medium when the plasma membrane is ruptured. In the present study, 10  $\mu$ l of culture medium was taken for the detection of LDH release using an LDH cytotoxicity assay kit (Nanjing Jiancheng Bioengineering Institute, Nanjing, China) according to the manufacturer's instruction. A microplate reader was used to measure the absorbance at 490 nm.

### Analysis of caspase-3 activity

The caspase-3/7 activities were measured by using a Caspase-Glo 3/7 assay kit (Promega, Madison, USA) according to the manufacturer's instructions as previously reported [25]. The luminescence was measured after 3 h of incubation with the caspase substrate.

### Total RNA extraction and qRT-PCR

Total RNA was extracted from cells and cardiac tissues by using Trizol reagent (Invitrogen, Carlsbad, USA) according to manufacturer's protocol. Total RNA (0.5  $\mu$ g) was reverse-transcribed by using the TransScript reverse transcriptase (TransGen Biotech, Beijing, China) to obtain cDNA. The mRNA levels of *Bax*, *Bcl2*, and *p53* were determined using SYBR Green I incorporation method on fast LightCycler 96 Real Time PCR system (Roche). The levels of mRNA were calculated using the  $2^{-\Delta\Delta CT}$  method. The relative data were determined

by using default threshold settings and the mean CT was determined from the duplicate PCRs. Primers used are listed in Table 1.

### Western blot analysis

Proteins were extracted from heart tissues and primary cultured cardiomyocytes according to standard protocols. Tissues or cell samples were lysed in RIPA lysis buffer containing the complete protease inhibitor (Roche). Protein concentrations were determined using a BCA Protein Assay kit (Pierce, Rockford, USA). The protein samples were subject to SDS-PAGE and transferred to NC membranes (Millipore, Billerica, USA). The NC membranes were blocked with 5% nonfat milk and incubated with the primary antibodies against iASPP (1:1000, 18590-1-AP; Proteintech, Rosemont, USA), Bax (1:1000, 60267-1-1g; Proteintech), Bcl2 (1:1000, 3498s; Cell Signaling Technology, Beverly, USA), P53 (1:1000, 2524s, Cell Signaling Technology), and  $\beta$ -actin (1:10,000, 66009-1-1g; Proteintech) overnight at 4°C. After that, the membranes were rinsed with Tris-buffered saline with Tween 20 buffer and incubated with the corresponding secondary antibodies (LI-COR Biosciences, Lincoln, USA). After extensive wash, the membranes were scanned by Imaging System (LI-COR Biosciences). The relative optical density of protein bands was measured after subtracting the film background. Protein levels were normalized to that of  $\beta$ -actin which is a loading control.

### Statistical analysis

Data are expressed as the mean  $\pm$  SEM. Statistical analysis between groups were done by unpaired Student's *t*-test. For multiple comparisons, one-way analysis of variance (ANOVA) was used, followed by Tukey's post-hoc analysis. All the experiments were repeated at least three times. GraphPad Prism 7.0 was used for statistical analyses. A  $P < 0.05$  was considered statistically significant.

## Results

### iASPP expression is significantly suppressed after MI

Early studies showed that iASPP is ubiquitously expressed in tissues, including cardiac tissue [26]. Thus, we firstly measured the expression level of iASPP in heart tissues of mice after MI surgery. The protein level of iASPP was significantly decreased 24 h after MI compared with that in sham controls (Fig. 1A). Consistent with the *in vivo* results, the protein level of iASPP was also significantly decreased in NMCs after 12 h of treatment with 200 nM  $H_2O_2$  *in vitro* (Fig. 1B). These data indicated that iASPP might be involved in myocardial ischemia injury.

### iASPP overexpression protects the heart from MI injury

A mouse model of MI was used to study the role of iASPP in cardiac injury. Adeno-associated virus (AAV-NC and AAV-iASPP) were introduced to mice by injecting into the tail vein 2 weeks before MI surgery. Overexpression of iASPP in the heart tissues was confirmed by western blot analysis (Fig. 2A). Echocardiography was performed to confirm myocardial damage after 24 h of LAD ligation. The left

**Table 1. Sequence of primers used for qRT-PCR**

| Gene           | Forward (from 5' to 3') | Reverse (from 5' to 3') |
|----------------|-------------------------|-------------------------|
| <i>BAX</i>     | CCAAGAAGCTGAGCGAGTGTC   | TGAGGACTCCAGCCACAAAGA   |
| <i>Bcl2</i>    | CTGGGCGAACAGGGTACGA     | ATGACCCACCGAACTCAA      |
| <i>p53</i>     | CCTCCTCAGCATCTTATCC     | ACAAACACGCACCTCAAA      |
| $\beta$ -Actin | GGCGGCACCACCATGTACCCT   | AGGGGCCGACTCGTCATACT    |

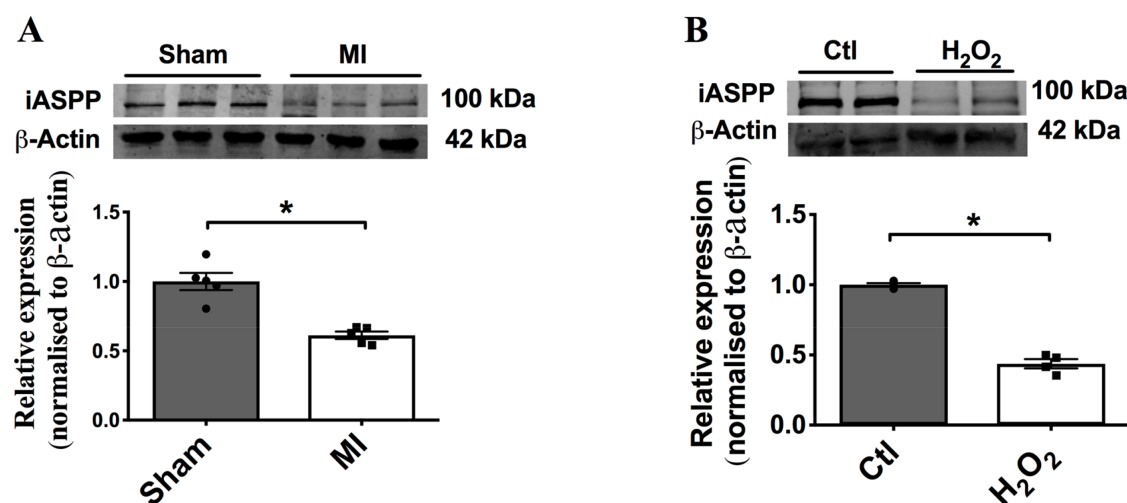


**Figure 1. iASPP was significantly downregulated after MI and in  $H_2O_2$ -treated cardiomyocytes** (A) iASPP level in cardiac tissue of MI mice.  $n=5$ .  $\beta$ -Actin served as a loading control. \* $P < 0.05$  vs Sham. (B) iASPP level in NMCMs with or without the treatment with 200 nM hydrogen peroxide.  $n=4$ . Ctl, Control. \* $P < 0.05$  vs Ctl.

ventricular EF and FS were reduced in MI mice than sham controls, which were alleviated by AAV-iASPP injection (Fig. 2B). The TTC assay showed that overexpression of iASPP significantly decreased the infarct size after MI compared with that of the mice receiving control vector (Fig. 2C). As an important sign of cell damage, the LDH release of cardiomyocytes was measured. The results showed that after MI, the LDH release of iASPP overexpression mice was decreased compared with the control group (Fig. 2D). To date, it is known that cardiomyocyte apoptosis plays an important role in ischemic myocardial damage. Here, we tried to find out whether the restoration of cardiac function by iASPP overexpression is associated with cardiomyocyte apoptosis. Western blot analysis results showed that overexpression of iASPP downregulated the level of Bax, a pro-apoptotic protein, and increased the expression of Bcl2 in MI mice (Fig. 2E,F). Since iASPP works through repressing p53 in cancer cells, we further tested the influence of iASPP on p53 in myocardial tissues. Consistently, p53 level was increased in the hearts of MI mice, which was inhibited by overexpression of iASPP (Fig. 2G). Intriguingly, the TUNEL staining also showed less apoptotic cardiomyocytes in MI mice with iASPP overexpression than in MI controls (Fig. 2H). These findings suggested that overexpression of iASPP causes a protective effect after MI.

#### iASPP overexpression mitigates $H_2O_2$ -induced cardiomyocyte apoptosis *in vitro*

To further confirm the cardioprotective effects of iASPP, we performed *in vitro* experiments to test the influence of iASPP on cardiomyocyte apoptosis induced by  $H_2O_2$ . Overexpression of iASPP in the cardiomyocytes was confirmed by western blot analysis (Fig. 3A). Treatment of cardiomyocytes with 200 nM  $H_2O_2$  leads to an upregulation of pro-apoptotic marker Bax and downregulation of anti-apoptotic protein Bcl2, which were reversed by overexpression of iASPP (Fig. 3B,C). The effect of iASPP overexpression on  $H_2O_2$ -exposed cardiomyocytes was further assessed by TUNEL staining and caspase-3 activity assay. The results showed that the introduction of iASPP significantly reduced the TUNEL-positive cells and caspase-3 activity after  $H_2O_2$  exposure (Fig. 3D,E). To investigate the changes of apoptosis-associated protein expressions after MI, the

mRNA levels were detected by qRT-PCR. Consistent with the protein expressions, the mRNA levels of Bax and p53 were upregulated after MI, while the level of anti-apoptotic protein Bcl2 was down-regulated. All these changes were reversed by iASPP overexpression (Fig. 3F-H).

#### iASPP deficiency deteriorates cardiac injury induced by MI

Since iASPP overexpression exhibits a cardioprotective effect, we went on to explore whether knockdown of iASPP in hearts has the opposite effect. Successful knockdown of iASPP in the heart was confirmed by western blot analysis (Fig. 4A). Reduction of EF and FS after MI surgery was detected by echocardiography, which was further decreased by iASPP knockdown (Fig. 4B). The TTC assay showed that knockdown of iASPP significantly increased the infarct size after MI for 24 h compared with that of the mice receiving control vector (Fig. 4C). In addition, iASPP deficiency significantly increased the ratio of TUNEL-positive cardiomyocytes (Fig. 4D). These results indicated that iASPP deficiency contributes to the aggravation of MI.

#### iASPP knockdown exacerbates $H_2O_2$ -induced cardiomyocyte apoptosis *in vitro*

Next, we investigated whether iASPP deficiency can influence cardiomyocyte apoptosis *in vitro*. Western blot analysis showed successful knockdown of iASPP in cardiomyocytes after transfection with the siRNA for iASPP (Fig. 5A). The TUNEL staining indicated that  $H_2O_2$ -induced cardiomyocyte apoptosis was significantly increased after transfection with the siRNA for iASPP (Fig. 5B,G). iASPP knockdown in cardiomyocytes further enhanced the activity of caspase-3 in  $H_2O_2$ -treated cardiomyocytes (Fig. 5C). The mRNA levels of Bax and p53 were upregulated in cardiomyocytes exposed to  $H_2O_2$ , which was further increased by the siRNA for iASPP (Fig. 5D-F). These data demonstrated that iASPP deficiency could exacerbate  $H_2O_2$ -induced cardiomyocyte apoptosis.



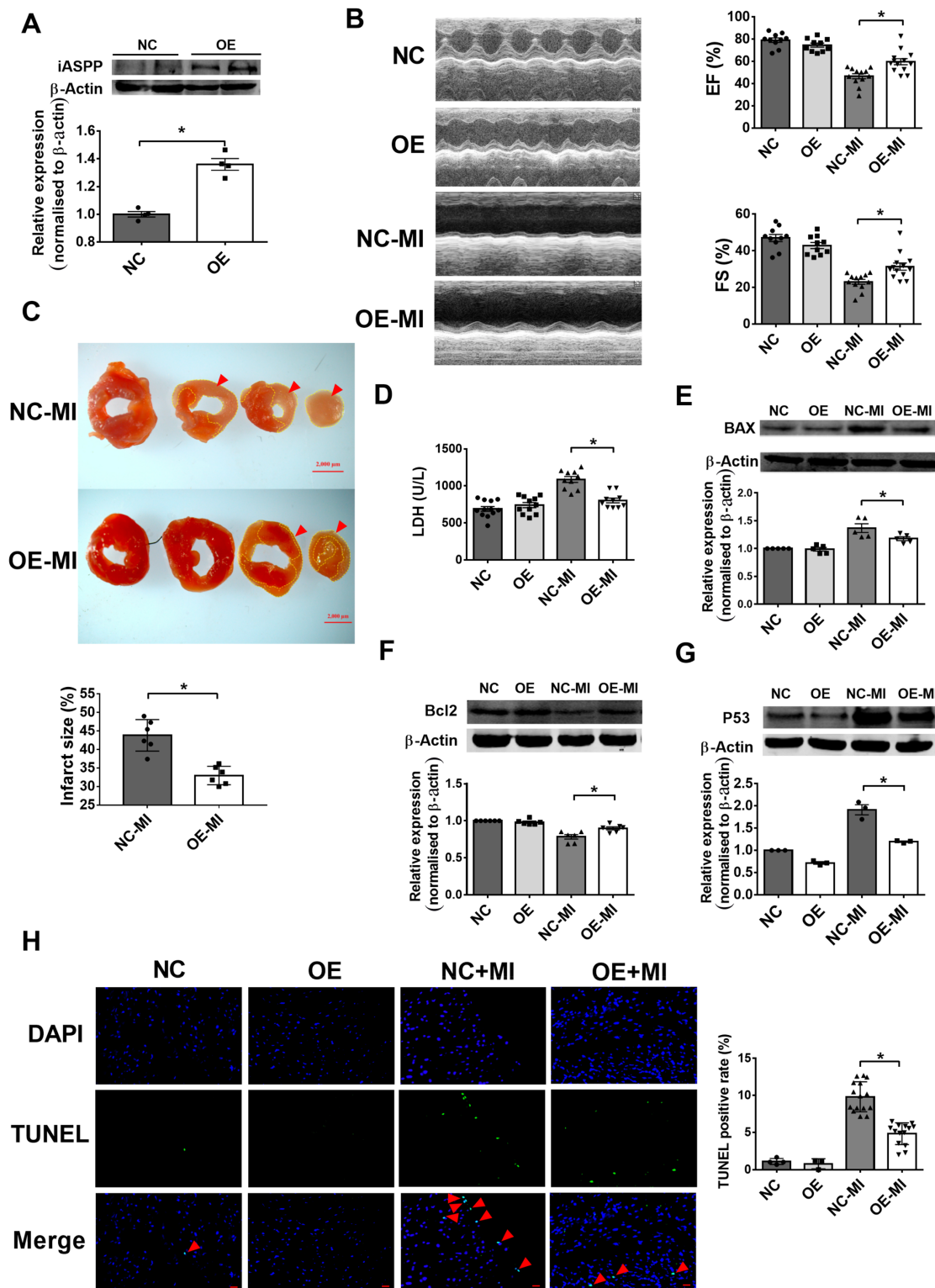


**Figure 2. iASPP overexpression attenuated apoptosis after MI** (A) Confirmation of iASPP overexpression (OE) 2 weeks after the injection of adeno-associated virus 9 through the tail vein.  $n = 10$ . NC, negative control; OE, overexpression of iASPP. (B) Cardiac function evaluated by echocardiography.  $n = 10$ . EF, ejection fraction; FS, fractional shortening. NC-MI, NC mice subjected to myocardial infarction surgery; OE-MI, OE mice subjected to myocardial infarction surgery. (C) Representative images of left ventricular (LV) sections from iASPP overexpression (OE-MI) and negative control (NC-MI) vector-injected mice 24 h after MI. The slices were stained with 2,3,5-triphenyltetrazolium chloride. The white zone indicates the infarcted region. The quantitative assessment of infarct size is shown lower.  $n = 6$ . (D) The release of lactate dehydrogenase (LDH).  $n = 10$ . (E–G) Western blots and quantitative results of apoptosis-related protein expression levels represented in four groups.  $n = 3$ –5. (H) TUNEL assay was performed in iASPP (OE) or control vector-injected (NC) mice with and without surgery. The arrows show TUNEL-positive cells. The bar graph indicates the number of TUNEL-positive cells. Scale bar = 20  $\mu$ m. Data are shown as the mean  $\pm$  SEM from at least three independent experiments. \*  $P < 0.05$  vs NC or NC-MI; ns, no significance.

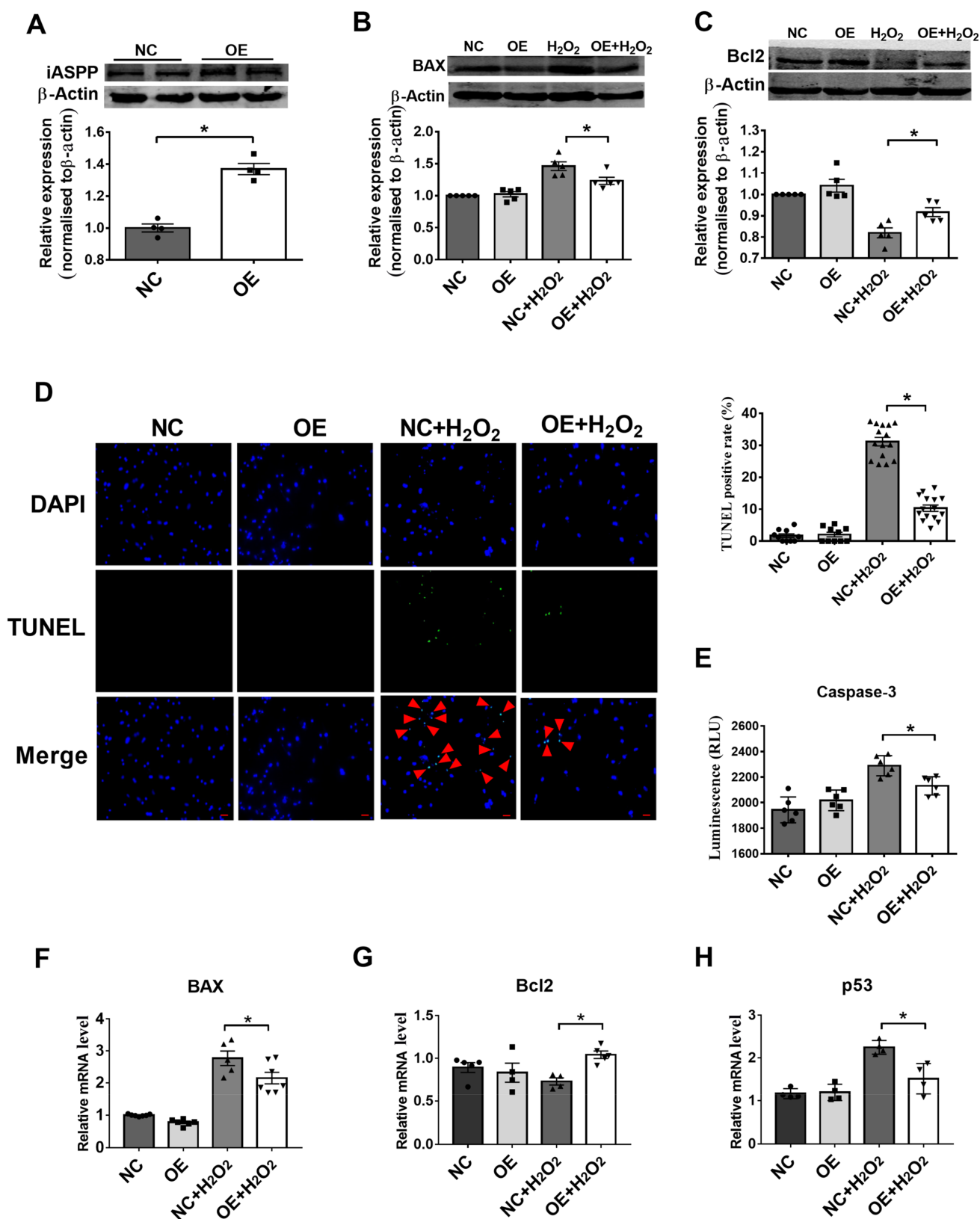


**Figure 3. iASPP overexpression reduced H<sub>2</sub>O<sub>2</sub>-induced cardiomyocyte apoptosis *in vitro*** (A) Overexpression of iASPP in NMCMs  $n=4$ . NC, negative control; OE, overexpression. (B,C) Representative western blots and statistical analysis of Bax and Bcl2 levels.  $n=5$ . (D) Representative images of TUNEL-stained NMCMs after H<sub>2</sub>O<sub>2</sub> exposure. The arrows show TUNEL-positive cells. The bar graph indicates the number of TUNEL-positive cells. Scale bar = 20  $\mu$ m. (E) Caspase-3 activity.  $n=6$ . (F–H) Relative mRNA levels of apoptosis-related proteins in cardiomyocytes.  $n=4$ . Data are shown as the mean  $\pm$  SEM from at least three independent experiments. \* $P<0.05$  vs NC or NC + H<sub>2</sub>O<sub>2</sub>.

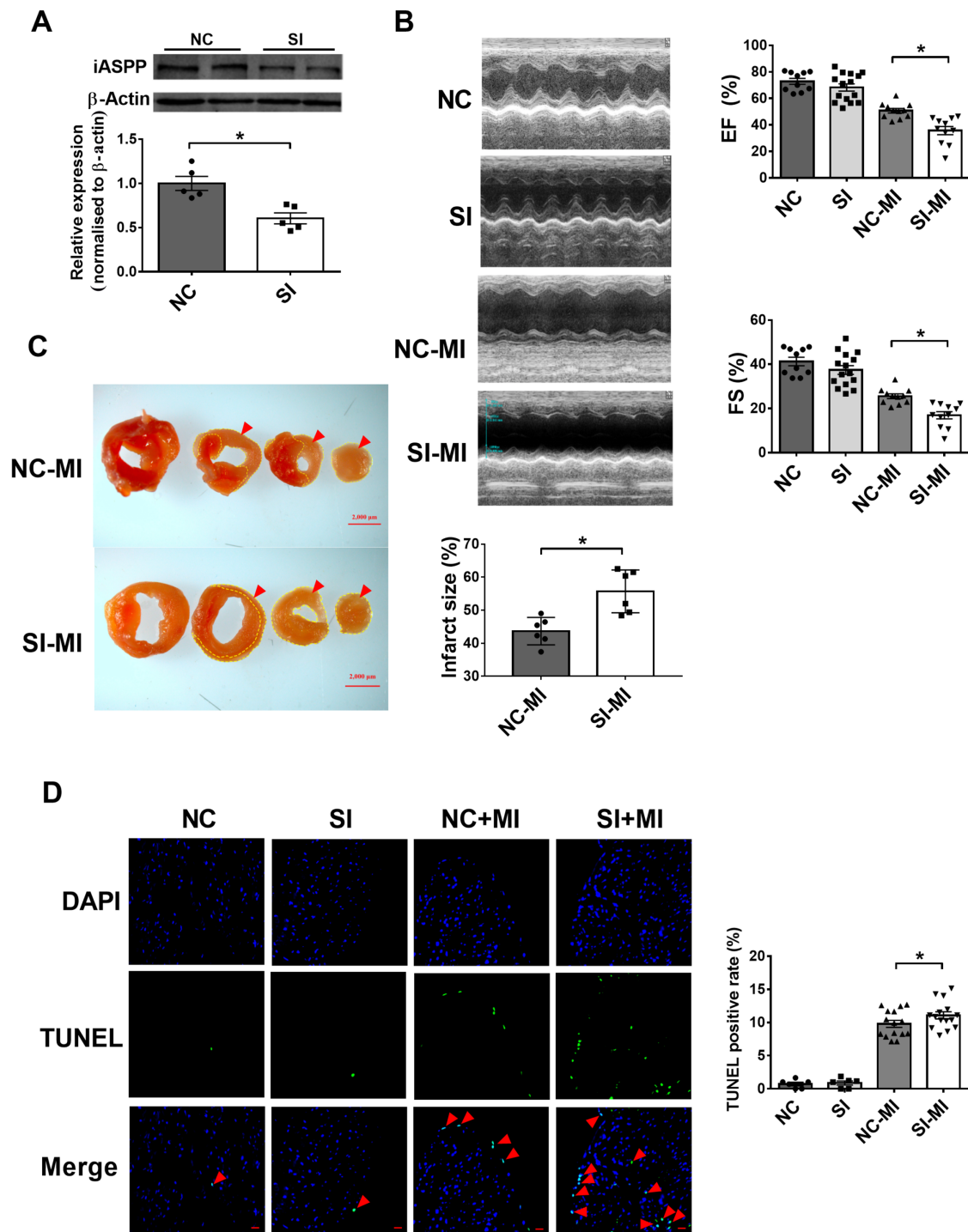


**Figure 4. iASPP deficiency increased apoptosis after MI *in vivo*** (A) Verification of iASPP knockdown in hearts of mice.  $n=5$ . NC, negative control; SI, AAV9 carrying siRNA of iASPP. (B) Cardiac function evaluated by echocardiography.  $n=10$ . EF, ejection fraction; FS, fractional shortening. NC-MI, NC mice subjected to myocardial infarction surgery; SI-MI, SI mice subjected to myocardial infarction surgery. (C) Representative illustrations of infarct size as stained by TTC in two groups (NC-MI, negative control and SI-MI, siRNA knockdown after MI). The white zone indicates the infarcted area. The quantitative assessment of infarct size is shown lower.  $n=6$ . (D) TUNEL assay performed in iASPP (SI) or control vector-injected (NC) groups with or without surgery. The arrows show TUNEL-positive cells. The bar graph indicates the number of TUNEL-positive cells. Scale bar = 20  $\mu$ m. Data are shown as the mean  $\pm$  SEM from at least three independent experiments. \* $P < 0.05$  vs NC or NC-MI.

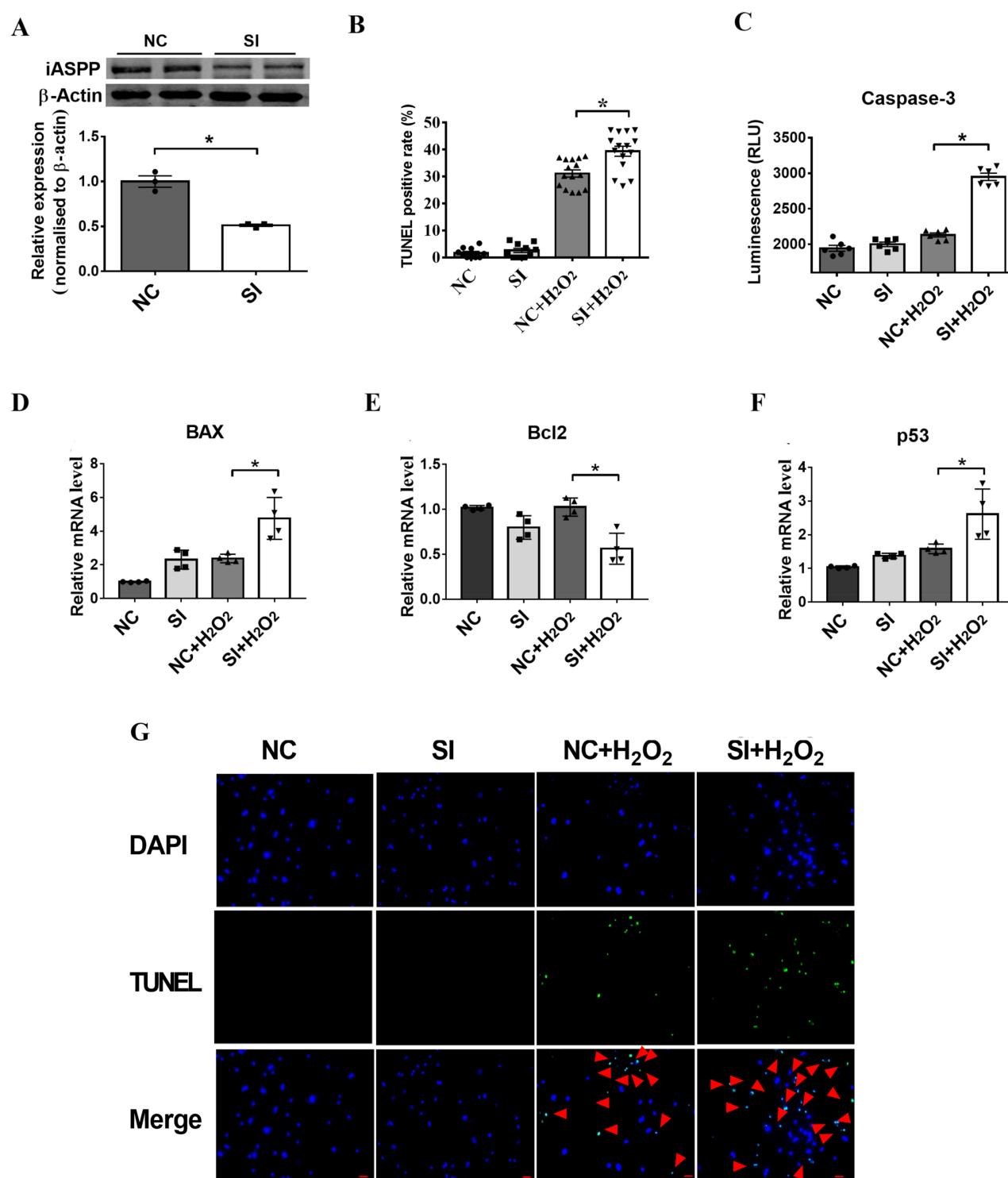


**Figure 5.** iASPP knockdown aggravates H<sub>2</sub>O<sub>2</sub>-induced cardiomyocyte apoptosis *in vitro* (A) Knockdown of iASPP in NMCMs.  $n=3$ . NC, negative control; SI, siRNA of iASPP. (B,G) Representative images of TUNEL-stained NMCMs after H<sub>2</sub>O<sub>2</sub> exposure (G). The arrows show TUNEL-positive cells. The bar graph indicates the number of TUNEL-positive cells. Scale bar = 20  $\mu$ m. (B) Represents the statistical data of (G). (C) Caspase-3 activity.  $n=6$ . (D–F) Relative mRNA levels of apoptosis-related proteins in cardiomyocytes. Data are shown as the mean  $\pm$  SEM from at least three independent experiments. \* $P < 0.05$  vs NC or NC + H<sub>2</sub>O<sub>2</sub>.



## Discussion

Previous studies have shown the involvement of iASPP in the development of various cancers, while its role in the cardiomyocytes remains unspecified. This is the first study to describe the beneficial effect of iASPP after MI. We found that iASPP is reduced in the mouse heart tissue following ischemic damage. iASPP overexpression after MI plays a protective role, while iASPP knockdown is detrimental in the development of cardiac ischemic injury.

MI is a process in which regional occlusion of the coronary arteries leads to a sharp decrease in oxygen nutrition in a certain area of the heart. Long-term hypoxia in large quantities or exposure to hydrogen peroxide on cardiomyocytes often leads to apoptosis. Moreover, several studies showed that apoptosis plays an important role in the development of cardiac dysfunction after MI [3]. This discovery led us to focus on the role of iASPP in H<sub>2</sub>O<sub>2</sub>-induced myocardial apoptosis. A previous study showed that anti-apoptotic therapy through genetic deletion of Bax was cardioprotective in MI [27]. Our *in vivo* and *in vitro* results confirmed that overexpression of iASPP exhibits cardioprotective effects, while inhibition of iASPP expression abolishes these effects, by regulating the expressions of apoptosis-associated proteins, including Bax and Bcl2. Therefore, iASPP overexpression may be an alternative therapeutic target for MI.

Caspase-3 has been proven as a frequently activated death protease that catalyzes the specific cleavage of many key cellular proteins, which ultimately leads to DNA fragmentation [28]. In this study, we found that the activity of caspase-3 was increased after MI, which was reduced by iASPP overexpression. In addition, Bax is known to target several genes of the p53 family and ASPP family [29]. Bax permeates the outer membrane of mitochondria and then releases apoptotic factors and cytochrome c into the cytosol, which promotes the activation of procaspase 9 and subsequent signaling as a response to various stimuli [30]. We also observed that iASPP can inhibit the increase of Bax expression. The influence of iASPP on caspase-3 and Bax confirmed the regulation of apoptosis by iASPP in cardiomyocytes.

As a critical tumor suppressor, p53 participates in cell cycle control, DNA repair, apoptosis, and cell stress responses as a transcription factor. The p53 protein can also penetrate mitochondria and activate the expressions of pro-apoptotic genes, as well as inhibit the expressions of anti-apoptotic genes, since it is associated with the mitochondrial internal apoptotic pathway [25,31]. As a consequence, p53 and pro-apoptotic proteins are transported to the mitochondria where they induce an increase in the permeability of mitochondrial membranes and the release of cytochrome c, and ultimately promote the activation of the caspase family [32]. We found that iASPP can inhibit p53 expression, which explains the mechanism of how iASPP prevents apoptosis, alleviates ischemic damage, and reduces the infarct size.

In summary, our data indicated that iASPP prevents myocardial apoptosis after MI by inhibiting p53 expression. Our findings provide insight into the roles of iASPP in myocardial injury and suggest that maintaining the balance between iASPP and p53 may provide potential targets for future clinical therapies.

## Funding

This work was supported by the grants from the National Key R&D Program of China (No. 2017YFC1307404 to Zhenwei Pan, Harbin Medical University), the National Natural Science Foundation of

China (No. 81730012 to Baofeng Yang, Harbin Medical University and No. 81870295 to Zhenwei Pan, Harbin Medical University), Funds for Distinguished Young Scholars of Heilongjiang Province (to Zhenwei Pan, Harbin Medical University), and Yu Weihai Excellent Youth Foundation of Harbin Medical University (No. 001000004 to Zhenwei Pan, Harbin Medical University).

## Conflict of Interest

The authors declare that they have no conflict of interest.

## References

1. Venardos KM, Perkins A, Headrick J, Kaye DM. Myocardial ischemia-reperfusion injury, antioxidant enzyme systems, and selenium: a review. *Curr Med Chem* 2007, 14: 1539–1549.
2. Heusch G, Rassaf T. Time to give up on cardioprotection? A critical appraisal of clinical studies on ischemic pre-, post-, and remote conditioning. *Circ Res* 2016, 119: 676–695.
3. Hojo Y, Saito T, Kondo H. Role of apoptosis in left ventricular remodeling after acute myocardial infarction. *J Cardiol* 2012, 60: 91–92.
4. Gareev I, Yang G, Sun J, Beylerli O, Chen X, Zhang D, Zhao B, *et al.* Circulating microRNAs as potential noninvasive biomarkers of spontaneous intracerebral hemorrhage. *World Neurosurg* 2020, 133: e369–e375.
5. Mohammadzadeh A, Mirza-Aghazadeh-Attari M, Hallaj S, Saei AA, Alivand MR, Valizadeh A, Yousefi B, *et al.* Crosstalk between P53 and DNA damage response in ageing. *DNA Repair (Amst)* 2019, 80: 8–15.
6. Rahimi A, Lee YY, Abdella H, Doerflinger M, Gangoda L, Srivastava R, Xiao K, *et al.* Role of p53 in cAMP/PKA pathway mediated apoptosis. *Apoptosis* 2013, 18: 1492–1499.
7. Cregan SP, Fortin A, MacLaurin JG, Callaghan SM, Cecconi F, Yu SW, Dawson TM, *et al.* Apoptosis-inducing factor is involved in the regulation of caspase-independent neuronal cell death. *J Cell Biol* 2002, 158: 507–517.
8. Chikh A, Sanza P, Raimondi C, Akinduro O, Warnes G, Chiorino G, Byrne C, *et al.* iASPP is a novel autophagy inhibitor in keratinocytes. *J Cell Sci* 2014, 127: 3079–3093.
9. Notari M, Hu Y, Koch S, Lu M, Ratnayaka I, Zhong S, Baer C, *et al.* Inhibitor of apoptosis-stimulating protein of p53 (iASPP) prevents senescence and is required for epithelial stratification. *Proc Natl Acad Sci USA* 2011, 108: 16645–16650.
10. Xiong S, Van Pelt CS, Elizondo-Fraire AC, Fernandez-Garcia B, Lozano G. Loss of Mdm4 results in p53-dependent dilated cardiomyopathy. *Circulation* 2007, 115: 2925–2930.
11. Bergamaschi D, Samuels Y, O'Neil NJ, Trigiant G, Crook T, Hsieh JK, O'Connor DJ, *et al.* iASPP oncoprotein is a key inhibitor of p53 conserved from worm to human. *Nat Genet* 2003, 33: 162–167.
12. Laska MJ, Vogel UB, Jensen UB, Nexø BA. p53 and PPP1R13L (alias iASPP or RAI) form a feedback loop to regulate genotoxic stress responses. *Biochim Biophys Acta* 2010, 1800: 1231–1240.
13. Chen J, Xie F, Zhang L, Jiang WG. iASPP is over-expressed in human non-small cell lung cancer and regulates the proliferation of lung cancer cells through a p53 associated pathway. *BMC Cancer* 2010, 10: 694.
14. Liu ZJ, Cai Y, Hou L, Gao X, Xin HM, Lu X, Zhong S, *et al.* Effect of RNA interference of iASPP on the apoptosis in MCF-7 breast cancer cells. *Cancer Invest* 2008, 26: 878–882.
15. Lu B, Guo H, Zhao J, Wang C, Wu G, Pang M, Tong X, *et al.* Increased expression of iASPP, regulated by hepatitis B virus X protein-mediated NF-kappaB activation, in hepatocellular carcinoma. *Gastroenterology* 2010, 139: 2183–2194.
16. Nexø BA, Vogel U, Olsen A, Nyegaard M, Bukowy Z, Rockenbauer E, Zhang X, *et al.* Linkage disequilibrium mapping of a breast cancer susceptibility locus near RAI/PPP1R13L/iASPP. *BMC Med Genet* 2008, 9: 56.
17. Zhang X, Wang M, Zhou C, Chen S, Wang J. The expression of iASPP in acute leukemias. *Leukemia Res* 2005, 29: 179–183.

18. Simpson MA, Cook RW, Solanki P, Patton MA, Dennis JA, Crosby AH. A mutation in NfκappaB interacting protein 1 causes cardiomyopathy and woolly haircoat syndrome of Poll Hereford cattle. *Anim Genet* 2009, 40: 42–46.
19. Whittington RJ, Cook RW. Cardiomyopathy and woolly haircoat syndrome of Poll Hereford cattle: electrocardiographic findings in affected and unaffected calves. *Aust Vet J* 1988, 65: 341–344.
20. Herron BJ, Rao C, Liu S, Laprade L, Richardson JA, Olivier E, Semarian C, *et al.* A mutation in NFκB interacting protein 1 results in cardiomyopathy and abnormal skin development in wa3 mice. *Hum Mol Genet* 2005, 14: 667–677.
21. Ju CH, Wang XP, Gao CY, Zhang SX, Ma XH, Liu C. Blockade of KCa3.1 attenuates left ventricular remodeling after experimental myocardial infarction. *Cell Physiol Biochem* 2015, 36: 1305–1315.
22. Kim JO, Park JH, Kim T, Hong SE, Lee JY, Nho KJ, Cho C, *et al.* A novel system-level approach using RNA-sequencing data identifies miR-30-5p and miR-142a-5p as key regulators of apoptosis in myocardial infarction. *Sci Rep* 2018, 8: 14638.
23. Borlaug BA, Paulus WJ. Heart failure with preserved ejection fraction: pathophysiology, diagnosis, and treatment. *Eur Heart J* 2011, 32: 670–679.
24. Long X, Boluyt MO, Hipolito ML, Lundberg MS, Zheng JS, O'Neill L, Cirielli C, *et al.* P53 and the hypoxia-induced apoptosis of cultured neonatal rat cardiac myocytes. *J Clin Invest* 1997, 99: 2635–2643.
25. Li S, Shi G, Yuan H, Zhou T, Zhang Q, Zhu H, Wang X. Abnormal expression pattern of the ASPP family of proteins in human non-small cell lung cancer and regulatory functions on apoptosis through p53 by iASPP. *Oncol Rep* 2012, 28: 133–140.
26. Dedeic Z, Sutendra G, Hu Y, Chung K, Slee EA, White MJ, Zhou FY, *et al.* Cell autonomous role of iASPP deficiency in causing cardiocutaneous disorders. *Cell Death Differ* 2018, 25: 1289–1303.
27. Hochhauser E, Cheporko Y, Yasovich N, Pinchas L, Offen D, Barhum Y, Pannet H, *et al.* Bax deficiency reduces infarct size and improves long-term function after myocardial infarction. *Cell Biochem Biophys* 2007, 47: 11–20.
28. Porter AG, Janicke RU. Emerging roles of caspase-3 in apoptosis. *Cell Death Differ* 1999, 6: 99–104.
29. Wilson AM, Morquette B, Abdouh M, Unsain N, Barker PA, Feinstein E, Bernier G, *et al.* ASPP1/2 regulate p53-dependent death of retinal ganglion cells through PUMA and Fas/CD95 activation in vivo. *J Neurosci* 2013, 33: 2205–2216.
30. Czabotar PE, Lessene G, Strasser A, Adams JM. Control of apoptosis by the BCL-2 protein family: implications for physiology and therapy. *Nat Rev Mol Cell Biol* 2014, 15: 49–63.
31. Wawryk-Gawda E, Chylinska-Wrzos P, Lis-Sochocka M, Chlapek K, Bulak K, Jedrych M, Jodlowska-Jedrych B. P53 protein in proliferation, repair and apoptosis of cells. *Protoplasma* 2014, 251: 525–533.
32. Chen S, Wu J, Zhong S, Li Y, Zhang P, Ma J, Ren J, *et al.* iASPP mediates p53 selectivity through a modular mechanism fine-tuning DNA recognition. *Proc Natl Acad Sci USA* 2019, 116: 17470–17479.